Development of a Nonlinear 7 DOF Model for Multi-Axle Hitched Vehicles

Lucas Dudley

August 14, 2024

Abstract

In pursuit of more robust vehicle controllers for autonomous driving, comprehensive vehicle models which characterize a wider range of vehicle types are needed. This project aims to develop a vehicle model for hitched vehicles such as tractor-semitrailers, stretched buses, or generally speaking, vehicles with hitched implements. A nonlinear bicycle model was chosen as the framework for the coupled model which utilizes the Dugoff coupled tire model to characterize combined lateral and longitudinal loads. Independent wheel velocities are also solved for allowing a variable longitudinal velocity which are determined via slip-ratios. While the equations of motion outlined here can be solved through a variety of different methods, MatLab Simulink was chosen as the test environment due to its robust numerical integrator and debugging tools.

1 Introduction

The objective of this research project was to develop a nonlinear vehicle model which captures the 2D planar dynamics of a hitched, multi-axle vehicle. While linear models have been outlined which capture the lateral dynamics of such systems, this model includes variable longitudinal velocity. To accomplish this, wheel velocities must be captured to characterize the slip ratios, and in turn capture the longitudinal forces.

This model is built upon the 'bicycle' model philosophy which reduces an axle to a single tire. This model does not account for weight transfer and assumes the normal loads at static equilibrium regardless of accelerations. For the low accelerations this model was intended to be used in, this was deemed acceptable.

2 Nonlinear Bicycle Model

To aid in the development of the multi-axle model, a non-coupled bicycle model was first developed. This allowed for key decisions, such as the tire model, to be chosen and tested outside of the complexity of the coupled model.

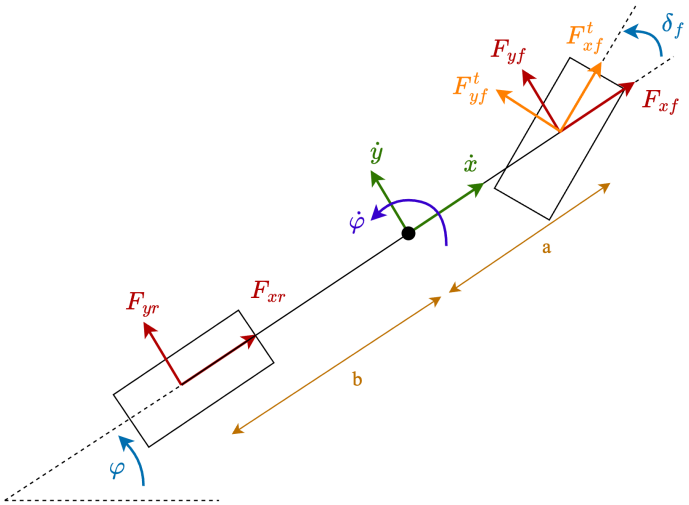

Figure 1: Graphical overview of bicycle model implemented.

2.1 Equations of Motion

A three degree of freedom bicycle model was implemented written compactly as:

$$\dot{\xi} = f(\xi(t), u(t)) \tag{1}$$

Where the output matrix $\xi = [\dot{x}, \dot{y}, \dot{\varphi}]'$ and the input matrix $u(t) = [\delta_f, t_b, t_a]'$ with $\dot{x}$ and $\dot{y}$ are the x-y components of velocity in the vehicle reference frame respectively and $\dot{\varphi}$ is the yaw-rate. Using Newtonian mechanics, it can be seen that the equations of motion for this system are defined as follows.

$$\sum F_x = m(\ddot{x} - \dot{y}\dot{\varphi}) = F_{xf} + F_{xr} - F_{drag} \tag{2}$$

$$\sum F_y = m(\ddot{y} + \dot{x}\dot{\varphi}) = F_{yf} + F_{yr} \tag{3}$$

$$\sum M_{cg} = I_{zz}\ddot{\varphi} = aF_{yf} - bF_{yr} \tag{4}$$

Where I_{zz} is the mass moment of inertia about the z-axis, m is the vehicle mass, a is the distance from the CG to the front axle, and b is the distance from the CG to the rear axle. Rearranging the equations for application in a time-domain block diagram yields:

$$\ddot{x} = \dot{y}\dot{\varphi} + \frac{F_{xf} + F_{xr} - F_{drag}}{m} \tag{5}$$

$$\ddot{y} = \frac{F_{yf} + F_{yr}}{m} - \dot{x}\dot{\varphi} \tag{6}$$

$$\ddot{\varphi} = \frac{aF_{yf} - bF_{yr}}{I_{zz}} \tag{7}$$

Equations 5-7 were used to develop the time-domain block diagram in Simulink seen in 2.

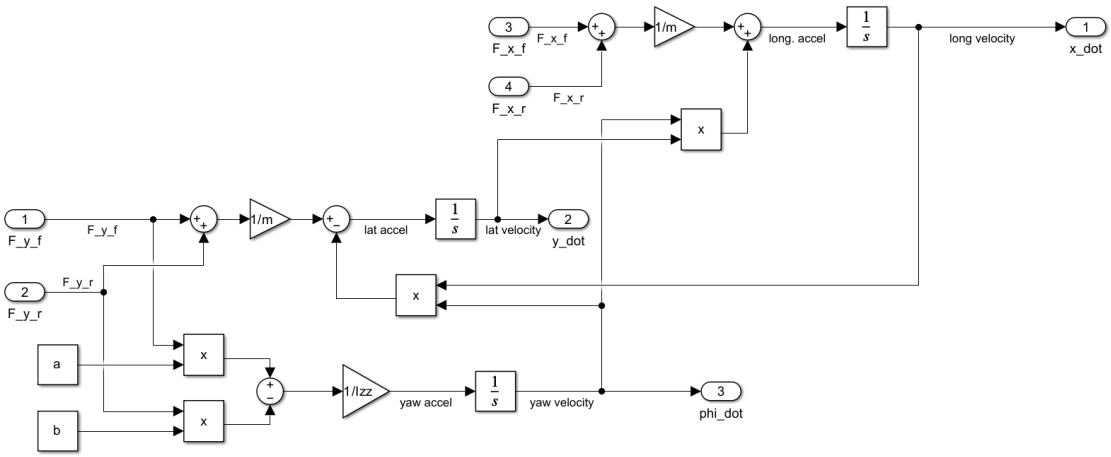

Figure 2: Vehicle EoM block diagram.

2.2 Tire Forces

Due to non-linear nature of this model utilizing a numerical integrator, a non-linear tire model which could represent combined lateral and longitudinal tire forces was implemented.

2.2.1 Slip Angle Calculation

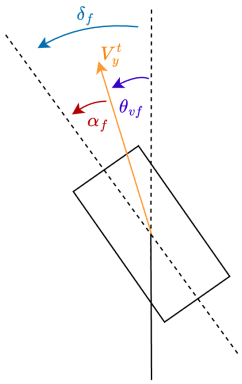

Figure 3: Slip angle derivation diagram.

The following relationship can be seen in 3. A similar relationship exists for the rear axle when $\delta_r = 0$.

$$\alpha_f = \delta_f - \theta_{vf}$$

$$\alpha_r = -\theta_{vr}$$

The geometric relationship can be used to find the angle of the velocity vector: $\theta_{v\star}$.

$$\tan(\theta_{vf}) = \frac{\dot{y} + a\dot{\varphi}}{\dot{x}}$$

$$\tan(\theta_{vr}) = \frac{\dot{y} - b\dot{\varphi}}{\dot{x}}$$

Which can in turn be used to find the front and rear slip angles:

$$\alpha_f = \delta_f - \arctan(\frac{\dot{y} + a\dot{\varphi}}{\dot{x}}) \tag{8}$$

$$\alpha_r = -\arctan(\frac{\dot{y} - b\dot{\varphi}}{\dot{x}}) \tag{9}$$

Where α_f and α_r are the front and rear slip angles respectively. Similarly, δ_f and δ_r are the front and rear steering inputs. From this point forward, is assumed in this model that $\delta_r = 0$.

Notice that there is a singularity in the slip angle calculation. To solve this, I assume the slip angle to be zero when $\dot{x}$ is zero as there can be no slip angle without longitudinal velocity.

2.2.2 Dugoff Tire Model

The Dugoff analytical tire model depends on model constants C_σ, C_α, and μ representing the longitudinal cornering stiffness, lateral cornering stiffness, and road-tire coefficient of friction respectively. The model depends on variable inputs: F_z, α, and σ for each axle representing the normal load on the tire, slip angle, and slip ratio.

The lateral and longitudinal tire forces with respect to the tire are found in terms of $f(\lambda)$ with the following equations:

$$F_x^t = C_\sigma \frac{\sigma_x}{1 + \sigma_x} f(\lambda) \tag{10}$$

$$F_y^t = C_\alpha \frac{\tan \alpha_x}{1 + \sigma_x} f(\lambda) \tag{11}$$

Where $f(\lambda)$ can be found with the following piece-wise function:

$$f(\lambda) = \begin{cases} (2 - \lambda)\lambda & \text{if } \lambda < 1 \\ 1 & \text{if } \lambda \geq 1 \end{cases} \tag{12}$$

Where lambda can be found using the following relationship:

$$\lambda = \frac{\mu F_z (1 + \sigma_x)}{2[(C_\sigma \sigma_x)^2 + (C_\alpha \tan(\alpha)^2]^{1/2}} \tag{13}$$

Below we can see a sample output of the Dugoff model as implemented. This model was chosen due to its computational simplicity while maintaining key features such as saturation drop in the SA-F_Y domain, and a non-linear relationship between F_X and F_Y seen in the figures below.

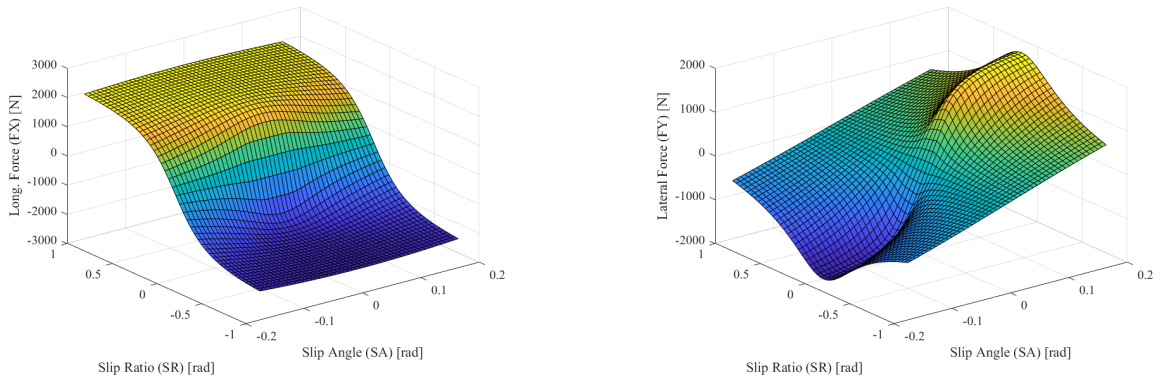

(a) Longitudinal Force output

(b) Lateral Force Output

Figure 4: Sample outputs with $C_\sigma = 15,000$, $C_\alpha = 10,000$ and $\mu = 0.5$

2.2.3 Tire Force Coordinate Transform

The Dugoff tire model outputs the tire forces F_x^t and F_y^t with respect to the tires inertial frame. However, the previously outlined EoM assume the tire forces coordinate system to by the vehicle x-y frame. As such, we must perform a simple transformation.

$$F_{x\star} = F_{x\star}^t cos(\delta_\star) - F_{y\star}^t sin(\delta_\star) \tag{14}$$

$$F_{y\star} = F_{x\star}^t sin(\delta_\star) + F_{y\star}^t cos(\delta_\star) \text{ where } \star \in [f, r] \tag{15}$$

2.2.4 Tire Normal Load

As assumption of the singe-track bicycle model is that there is no weight transfer, laterally or longitudinally, resulting in a constant normal load F_z. The normal load assumed in this model is found using the following equations:

$$F_{zf} = \frac{b}{(a+b)}mg \tag{16}$$

$$F_{zr} = \frac{a}{(a+b)}mg \tag{17}$$

2.2.5 Aerodynamic Forces

Aerodynamic drag and down-force are estimated in this model using constant coefficients of drag and lift. Note that side-force moments and ride height sensitivity are not considered.

$$F_d = \frac{1}{2}C_d\rho V^2 A \tag{18}$$

$$F_l = \frac{1}{2}C_l\rho V^2 A \tag{19}$$

Where ρ is the density of air, A is the frontal area, and $V = \dot{x}$.

2.3 Longitudinal Dynamics

2.3.1 Slip Ratio Calculation

The following equation can be used to find slip ratios when the vehicle is in motion. Notice the divide by zero singularities which is exist in the following formulae when the tangential wheel velocity or the vehicle velocity is zero.

$$\sigma_x = \begin{cases} \frac{r\omega_\star - V^t_{x\star}}{r\omega_\star} & \text{Acceleration} \\ \frac{r\omega_\star - V^t_{x\star}}{V^t_x} & \text{Braking} \end{cases} \tag{20}$$

2.3.2 Slip Ratio Singularity Control

As slip ratio is normalized to the wheel or ground velocity depending on the case, there exists a singularity when this is zero. Furthermore, due to the feedback needed to solve for slip ratio, an initialization statement is needed when departing rest for non-driven axles.

One can see that for the front, non-driven wheel, there exists a state where the vehicle is no longer at rest yet the slip ratio would be zero if there was not an initialization statement. This can be seen by examining how the rotational velocity, which is needed to be non-zero to have a slip ratio, is a function only of the tire force and braking torque. However, for a tire force to exists, there must be a slip ratio. Hence initialization is need when beginning from rest.

To combat these issues, the following cases were defined:

Conditions	Case	Justification
$\omega = 0$ and throttle $\neq 0$	$\sigma = \sigma_{inital}$	Initialization Statement
$r\omega = 0$	$\sigma = 0$	Prevents Braking Singularity
$V^t_x = 0$	$\sigma = 0$	Prevents Accel. Singularity
$r\omega > V^t_x$	Accel.	Satisfies SR Defn.
$r\omega < V^t_x$	Braking	Satisfies SR Defn.

Table 1: Slip Ratio Control

Where σ_{inital} was chosen as a small negative value which converged for all non-driven wheels.

2.3.3 Wheel Velocity Coordinate Transform

The slip ratio depends of the longitudinal velocity of the tire within the tires frame. Thus, it is necessary to transform the vehicle frame velocities to the tires frame. The following identities are true:

$$V_{yf} = \dot{y^t} + a\dot{\varphi^t}$$

$$V_{xf} = \dot{x^t}$$

Which can be used in conjunction with the following relationships:

$$V_{xf}^t = V_{yf} sin\delta_f + V_{xf} cost\delta_f \tag{21}$$

$$V_{xr}^t = \dot{x^t} \tag{22}$$

2.3.4 Wheel Dynamics

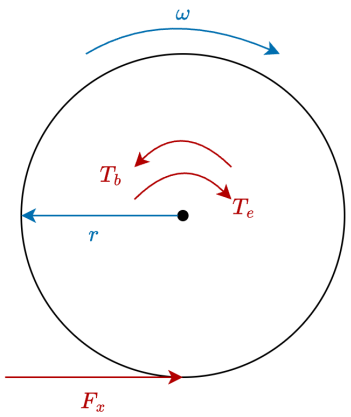

Figure 5: Forces and toques acting on the wheel

To determine the wheel velocity, a necessary input to calculate the slip ratio, Newtonian mechanics were used to find the angular acceleration which is integrated to find the angular velocity. The guiding equations for the wheel dynamics are as follows:

$$\sum M_{xf} = I_w \dot{\omega_f} = -rF_{xf}^t - T_{bf} \tag{23}$$

$$\sum M_{xr} = I_w \dot{\omega_r} = T_e - rF_{xr}^t - T_{br} \tag{24}$$

Where T_e is the engine torque, T_b is the braking torque, r is the wheel diameter, and I_w is the wheels moment of inertia.

2.3.5 Wheel Dynamics Logic

As outlined above and expanded upon in section 2.5.2, braking forces are modelled as a torque T_b. While this is a sufficient model when the vehicle is in motion, this model alone is not sufficient when the vehicle is at rest with a non-zero brake set-point at the wheel would begin rotating in the negative direction. To combat this, the following logic was implemented to recognize when the vehicle was at rest.

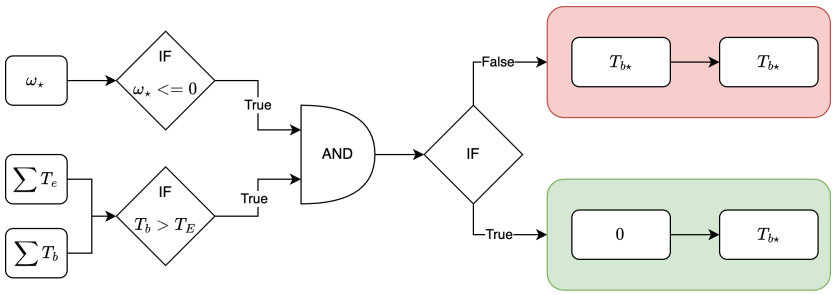

Figure 6: Logic for Braking Torque

Note that the simplifying assumption was made that the vehicle is at rest when the total sum of the braking torques is greater than the engine torque. This may not be true as the braking torques are not acting on the same body. However, it is sufficient for the majority of cases and was chosen for its simplicity and ability to remain in terms of torques, and not forces, thus avoiding slip ratios and the tire model.

Additionally, a delay block was added in the simulation environment to trigger the wheel rotation as zero for 20 time steps as opposed to strictly the current time step to reduce noise.

2.4 Global Coordinate Transformation

The final output of this model is a the global X-Y coordinate position. This is produced by integrating the global velocity components $\dot{X}$ and $\dot{Y}$. The following transformation from the vehicle frame to global frame is used:

$$\dot{X} = \dot{x}cos\varphi - \dot{y}sin\varphi \tag{25}$$

$$\dot{Y} = \dot{x}sin\varphi + \dot{y}cos\varphi \tag{26}$$

2.5 Simulation Method

2.5.1 Overview

MatLab Simulink was chosen as the simulation environment for the development of this model due to a plethora of debugging tools, a powerful numerical integrator and ease of development. The following figure outlines the general structure of the simulation environment, partitioning the system in a few key subsystems. Notice the feedback from the EoM block into the wheel dynamics and slip angle calculation blocks. This is a result of slip depending on the current vehicle state.

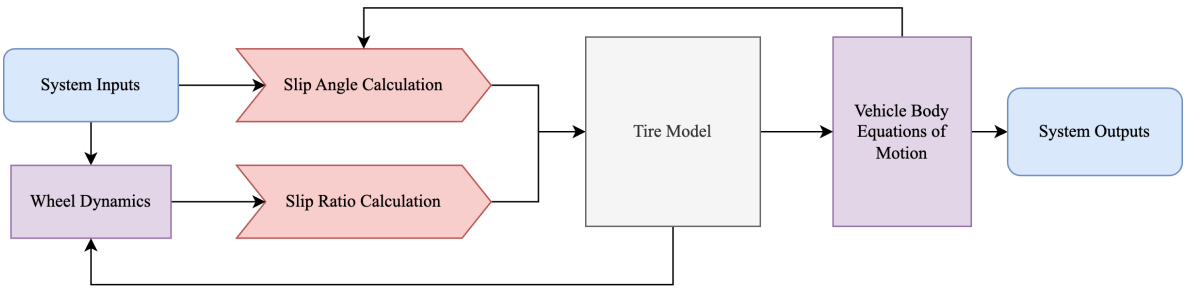

Figure 7: Simulation process flow chart.

The equations outlined above were then written into MatLab function files and linked to in the Simulink block diagram seen below.

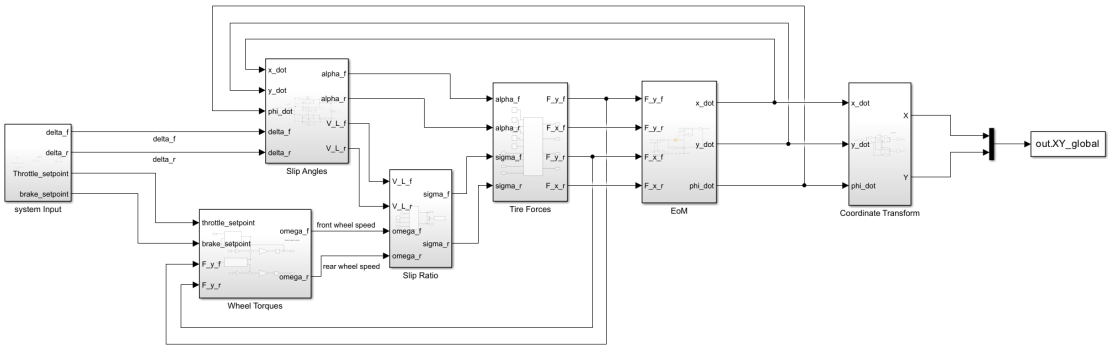

Figure 8: Simulink block diagram model overview.

2.5.2 Engine and Brake Torque Models

The engine torque T_e is the product of of a 1-D lookup table relating engine torque to engine speed and the throttle set point value [0:1]. This value is multiplied by the gear ratio and drive-train efficiency before being used in the wheel dynamics.

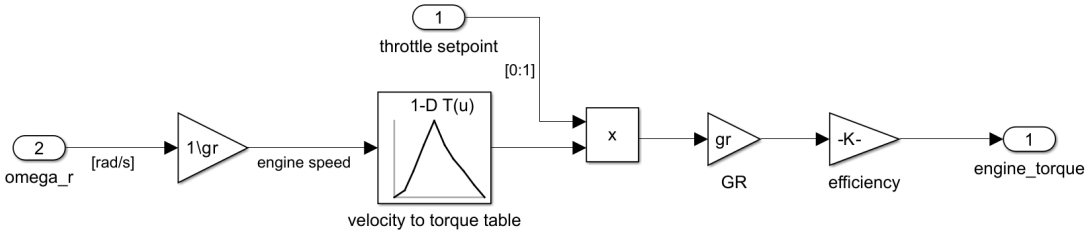

Figure 9: Engine model block diagram.

The brake torque T_b is solved for in a similar manner. A 1-D lookup table relating brake set point to braking torque is used before being multiplied by the brake bias to result in the final brake torque.

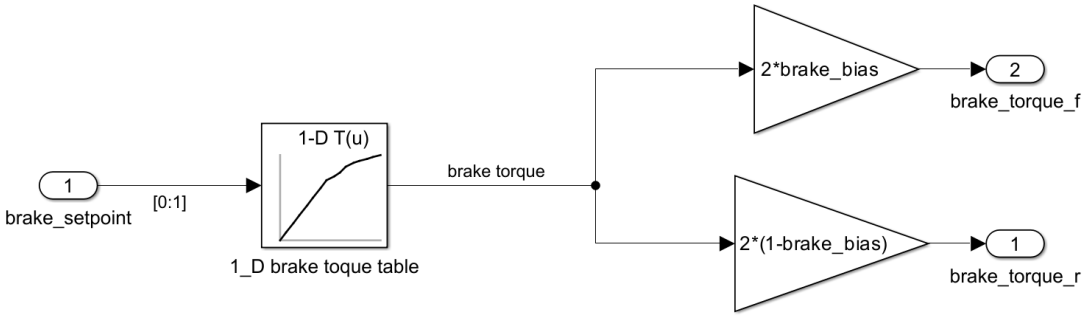

Figure 10: Brake model block diagram.

3 Multi-Axle Vehicle Model

3.1 Vehicle Architecture

The hitched multi-axle vehicle model is based on the same architecture as the nonlinear bicycle model outlined above. This model contains an additional degree of freedom: the angular velocity denoted as $\dot{\varphi}^i$. This is coupled to the bicycle model at the point H with a force coupling. The rear tire of the implement has a rotational degree of freedom allowing for longitudinal tire forces in addition to its own slip angle.

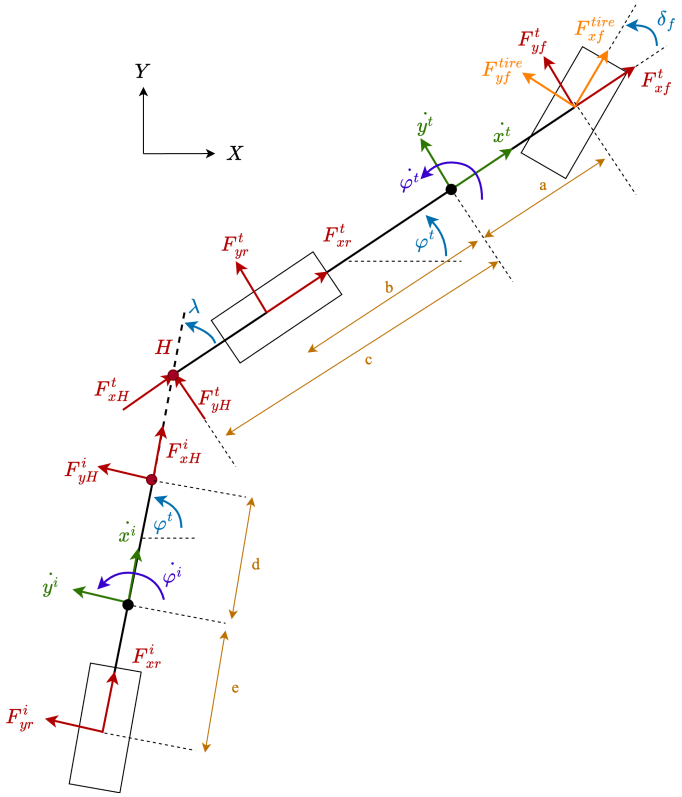

Figure 11: Graphical overview of hitched multi-axle vehicle model.

3.2 Vehicle Body Dynamics

The three degree of freedom vehicle body is defined by 3 equations of motion which are largely similar to those present on the bicycle model with an the additional forces from the hitch coupling present. The following equations can be used to solve the accelerations of the vehicle body.

$$\sum F_x^t = m^t(\ddot{x^t} - \dot{y^t}\dot{\varphi^t}) = F_{xf}^t + F_{xr}^t + F_{yH}^t \tag{27}$$

$$\sum F_y^t = m^t(\ddot{y^t} + \dot{x^t}\dot{\varphi^t}) = F_{yf}^t + F_{yr}^t + F_{xH}^t \tag{28}$$

$$\sum M_{cg}^t = I_{zz}^t\ddot{\varphi^t} = aF_{yf}^t - bF_{yr}^t - cF_{yH}^t \tag{29}$$

3.3 Implement Dynamics

While the implement has a single degree of freedom, its three equations of motion are used to determine the coupling force acting on the vehicle body. By rearranging for the force from the guiding equations and utilizing a velocity transformation from the vehicle CG, we can obtain the force at the hitch.

3.3.1 Lateral Dynamics

The following equation models the lateral dynamics of the implement:

$$\sum F^i_{yH} = m^i(\ddot{y^i} + \dot{x^i}\dot{\varphi^i}) = F^i_{yr} + F^i_{yH}$$

Which can be rearranged to solve for the unknown hitch forces:

$$F^i_{yH} = m^i(\ddot{y^i} + \dot{x^i}\dot{\varphi^i}) - F^i_{yr} \tag{30}$$

3.3.2 Longitudinal Dynamics

The longitudinal dynamics are similarly derived:

$$\sum F^i_{xH} = m^i(\ddot{y^i} - \dot{x^i}\dot{\varphi^i}) = F^i_{xr} + F^i_{xH}$$

Which when rearranged for the unknown hitch force yields:

$$F^i_{xH} = m^i(\ddot{y^i} - \dot{x^i}\dot{\varphi^i}) - F^i_{xr} \tag{31}$$

3.3.3 Rotational Dynamics

We can solve for the angular velocity about the pinned location H by utilizing the parallel axis theorem to find the new moment of inertia I_{pin}.

$$I_{pin} = I^i_{zz} + m^i d^2 \tag{32}$$

Summing the moments about the pin using taking CCW as positive:

$$\sum M^i_{pin} = I_{pin}\ddot{\varphi^i} = -F^i_y r(e+d)$$

When when rearranged into a form conducive to time domain block diagrams:

$$\ddot{\varphi^i} = \frac{-F^i_{yr}(e+d)}{I_{pin}} \tag{33}$$

3.4 Velocity Transform

To obtain the accelerations present at the CG of the implement body, a velocity transform is necessary. Numerical differentiation will then be used to find the accelerations which will be substituted into the implement EoMs.

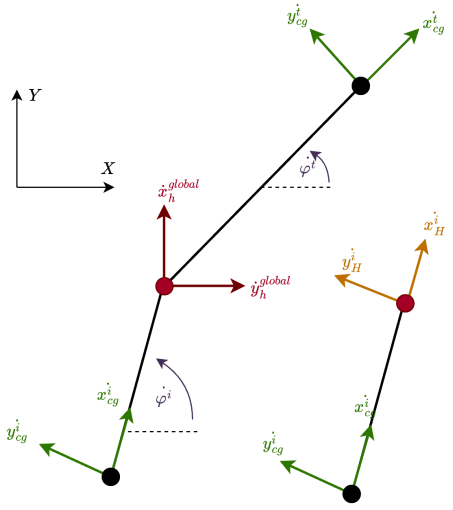

Figure 12: Velocity Transformation diagram

To perform the velocity transformation, we first transform the velocity at the vehicle CG from the vehicles frame to the global velocity at the hitch.

$$V_H^t = V_{CG}^t + V_H^{rel} \text{ where } V_H^{rel} = -\dot{\varphi} c \hat{j} \text{ which yields: } V_H^t = \dot{x^t}\hat{i} + (\dot{y^t} - \dot{\varphi^t} c)\hat{j}$$

We can then rotate to the global coordinate system.

$$\begin{bmatrix} \dot{x_H^{global}} \\ \dot{Y_H^{global}} \end{bmatrix} = \begin{bmatrix} \cos(\varphi^t) & -\sin(\varphi^t) \\ \sin(\varphi^t) & \cos(\varphi^t) \end{bmatrix} \begin{bmatrix} \dot{x^t} \\ \dot{y^t} - \dot{\varphi^t} c \end{bmatrix}$$

Which when expanded results in:

$$\dot{x}_H^{global} = \dot{x^t} \cos(\varphi^t) - (\dot{y^t} - \dot{\varphi^t} c) \sin(\varphi^t) \tag{34}$$

$$\dot{y}_H^{global} = \dot{x^t} \sin(\varphi^t) + (\dot{y^t} - \dot{\varphi^t} c) \cos(\varphi^t) \tag{35}$$

We can then utilize a rotation to find the velocity in the implements frame:

$$\begin{bmatrix} \dot{x_H^i} \\ \dot{Y_H^i} \end{bmatrix} = \begin{bmatrix} \cos(\varphi^i) & \sin(\varphi^i) \\ -\sin(\varphi^i) & \cos(\varphi^i) \end{bmatrix} \begin{bmatrix} \dot{x}_H^{global} \\ \dot{y}_H^{global} \end{bmatrix} \tag{36}$$

Finally, we must account for the component of lateral velocity which is a product of angular velocity:

$$\begin{bmatrix} \dot{x_{cg}^i} \\ \dot{Y_{cg}^i} \end{bmatrix} = \begin{bmatrix} \dot{x}_H^i \\ \dot{y}_H^i - \dot{\varphi^i} d \end{bmatrix} \tag{37}$$

3.5 Force Transform

To relate the hitch force from the implement frame to the vehicle frame, we first rotate the implement force F^i to the global frame. Since it is a clockwise rotation, we use R^T.

$$F^{global} = R^T F^i \text{ where } R^T = \begin{bmatrix} cos(\varphi^i) & sin(\varphi^i) \\ -sin(\varphi^i) & cos(\varphi^i) \end{bmatrix}$$

Which when expanded becomes:

$$F_x^{global} = F_x^i cos(\varphi^i) + F_y^i sin(\varphi^i) \tag{38}$$

$$F_y^{global} = -F_x^i sin(\varphi^i) + F_y^i cos(\varphi^i) \tag{39}$$

We now must rotate this global force vector counter-clockwise to the vehicle position. Since the force is a reaction force, it is negative:

$$F^t = -RF^{global} \text{ where } R^T = \begin{bmatrix} cos(\varphi^i) & -sin(\varphi^i) \\ sin(\varphi^i) & cos(\varphi^i) \end{bmatrix}$$

Which when expanded yields:

$$F_x^t = -F_x^{global} cos(\varphi^t) + F_y^{global} sin(\varphi^t) \tag{40}$$

$$F_y^t = -F_x^{global} sin(\varphi^t) - F_y^{global} cos(\varphi^t \tag{41}$$

3.6 Tire Forces

The tire forces F_{xr}^i and F_{yr}^i are calculated in much the same way as they are in the NL bicycle model. Slip angles and slip ratios are calculated before being the coupled Dugoff tire model is applied.

3.6.1 Slip Angles

The implement slip angle can be calculated using the implement CG velocities found earlier as follows:

$$\alpha_f^t = \delta_f - \arctan(\frac{\dot{y^t} + a\dot{\varphi^t}}{\dot{x^t}}) \tag{42}$$

$$\alpha_r^t = -\arctan(\frac{\dot{y^t} - b\dot{\varphi^t}}{\dot{x^t}}) \tag{43}$$

$$\alpha_r^i = -\tan(\frac{\dot{y^i} - e\dot{\varphi^i}}{\dot{x^i}}) \tag{44}$$

3.6.2 Wheel Dynamics

The guiding equations for the coupled model wheel dynamics were derived using Newtonian mechanics in the same way as NL Bicycle model.

$$\sum M_{xf}^t = I_w\dot{\omega_f^t} = -rF_{xf}^{tire} - T_{bf}^t \tag{45}$$

$$\sum M_{xr}^t = I_w\dot{\omega_r^t} = T_e - rF_{xr}^{tire} - T_{br}^t \tag{46}$$

$$\sum M_{xr}^i = I_w\dot{\omega_r^i} = -rF_{xr}^i - T_{br}^i \tag{47}$$

See section 2.3.4 covering wheel dynamics logic in the simulation environment.

3.6.3 Slip Ratios

$$\sigma_\star^t = \begin{cases} \frac{r\omega_\star - V_{x\star}^t}{r\omega_\star} & \text{Acceleration} \\ \frac{r\omega_\star - V_{x\star}^t}{V_x^t} & \text{Braking} \end{cases} \quad \text{for } \star \in [f, r]$$

Where the following relationships can be used to find $V_{x\star}^t$:

$$V_{xf}^t = (\dot{y} + a\dot{\varphi})sin\delta_f + \dot{x}cos\delta_f$$

$$V_{xr}^t = \dot{x}$$

Similarly, the slip ratio can be found for the implements rear wheel utilizing the velocity transform outlined earlier:

$$\sigma_r^i = \begin{cases} \frac{r\omega_r^i - \dot{x^i}}{r\omega_r^i} & \text{Acceleration} \\ \frac{r\omega_r^i - \dot{x^i}}{\dot{x^i}} & \text{Braking} \end{cases} \tag{48}$$

See section 2.3.2 covering Slip Ratio singularity control. The same initialization outlined was implemented in this model.

3.6.4 Tire Model

The same tire model which was used for the NL Bicycle model was implemented in this model, of which a summary of equations can be found below:

$$F_x^t = C_\sigma \frac{\sigma_x}{1 + \sigma_x} f(\lambda)$$

$$F_y^t = C_\alpha \frac{\tan\alpha_x}{1 + \sigma_x} f(\lambda)$$

$$f(\lambda) = \begin{cases} (2 - \lambda)\lambda & \text{if } \lambda < 1 \\ 1 & \text{if } \lambda \geq 1 \end{cases}$$

$$\lambda = \frac{\mu F_z(1 + \sigma_x)}{2[(C_\sigma\sigma_x)^2 + (C_\alpha \tan(\alpha)^2]^{1/2}}$$

3.7 Normal Loads

With the addition of the implement mass and another axle, the force balance become more involved.

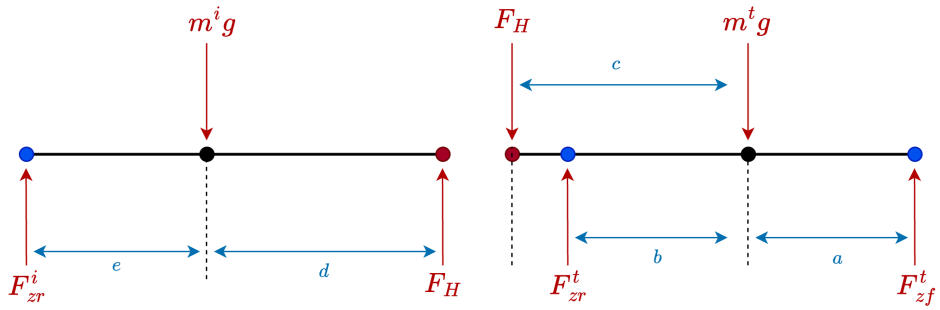

Figure 13: Force and moment balance diagram. XZ Plane

By summing the forces in the entire vehicle frame, summing the moments on the implement about point H and similarly summing the moments about the rear tire of the vehicle body, we obtain the following equations:

$$F_H = \frac{m^i g e}{e + d} \tag{49}$$

Which can be substituted into the following two equations:

$$F^t_f = \frac{m^t g b - F_H c}{a + b} \tag{50}$$

$$F^t_r = \frac{m^t g a + F_H (a + b}{a + b} \tag{51}$$

And then with all of the following substituted, we can find our last unknown:

$$F^i_r = m^i g - F_h \tag{52}$$

Note that neither longitudinal nor lateral weight transfer are accounted for in this model and these normal loads are assumed constant. Aerodynamic forces are also ignored in this model due to complexity of characterising CoP over two bodies.

3.8 Implement CG Global Coordinate Transform

While it is possible to integrate the implements CG velocities and perform a transformation to the global coordinate system, a geometric relationship was instead used, depending only on the output of a single integrator for the angular position, maintaining that the final position is geometrically possible given the vehicle parameters.

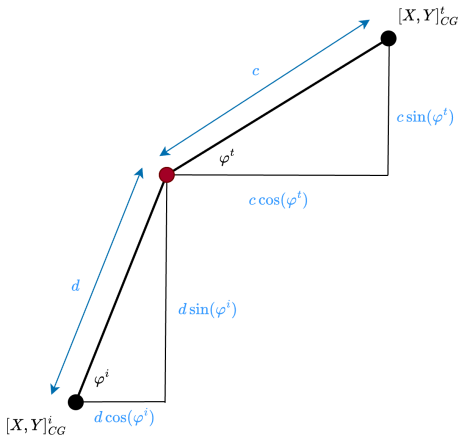

Figure 14: Geometric relationship between vehicle and implement CG

Using the above figure, it can be seen that the following transformation is true:

$$X^i = X^t - c\cos(\varphi^t) - d\cos(\varphi^i) \tag{53}$$

$$Y^i = Y^t - c\sin(\varphi^t) - d\sin(\varphi^i) \tag{54}$$

3.9 Simulation Method

The coupled model works in much the same way as the bicycle model. The same logic is applied to the wheel dynamics and the slip ratio and slip angles are calculated in the same way. However, the coupling of the two bodies takes place via the implement EoM. The accelerations at the Vehicle are calculated before those are transformed using the previous time steps value for the angular positions to find the accelerations at the implement CG. Similarly, the velocities are transformed to calculate the slips which then results in known tire forces

The known accelerations at the implement are used in combination with the tire forces to solve for the hitch force. This hitch forces, once rotated into the vehicles frame, is then used to update the vehicle body accelerations in the next time-step.

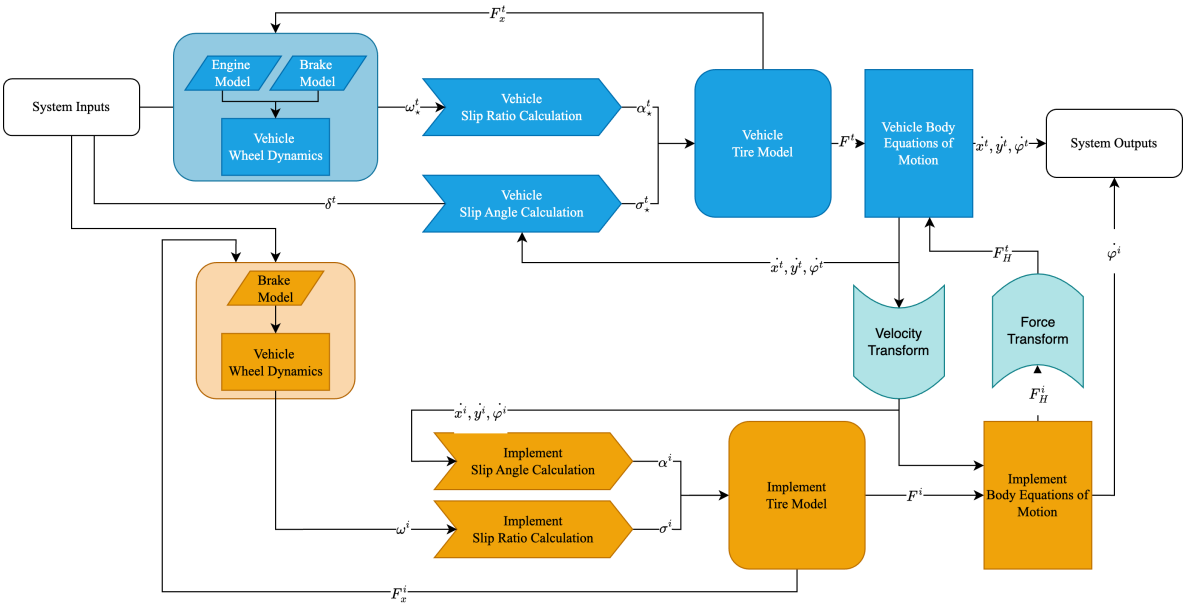

Figure 15: Simulation signal flow for coupled model

4 Simulation Results

Both the NL Bicycle model and Hitched-model were tested with a variety of simulation inputs:

4.1 Simulation Inputs

The following values were used in the following simulations:

Properties	Value
M^t	$400kg$
M^i	$200kg$
I^t_{zz}	$1000kg.m^2$
I^i_{zz}	$500kg.m^2$
$A[m]$	$0.8m$
$B[m]$	$1m$
$C[m]$	$0.8m$
$D[m]$	$0.5m$
$E[m]$	$1m$
$R[m]$	$0.25m$
$\mu[m]$	0.7
C_{alpha}	$30,000N/rad$
C_{sigma}	$8000N/rad$
I_{wheel}	$20kg.m^2$
$drivetrain_e$	0.8
Gear Ratio	1
Brake Bias	0.5
C_d	0.3
A	$2m^2$
ρ	$1.225kg/m^3$
CoP	0.4

Table 2: Simulations Parameters

4.2 Bicycle Model

4.2.1 Longitudinal Response

This simulation demonstrates the longitudinal dynamics and slip ratio control outlined in 2.3.2. The steering input is zero for the following simulation results. Here we can see the vehicle approach rest and maintain at rest with a non-zero braking set-point before accelerating from rest again when the engine torque exceeds the braking torque.

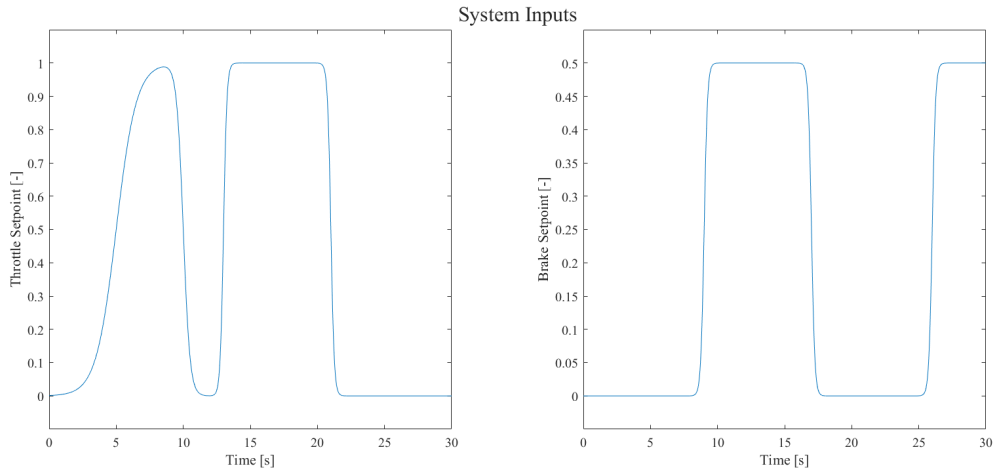

Figure 16: Bicycle Model System Inputs

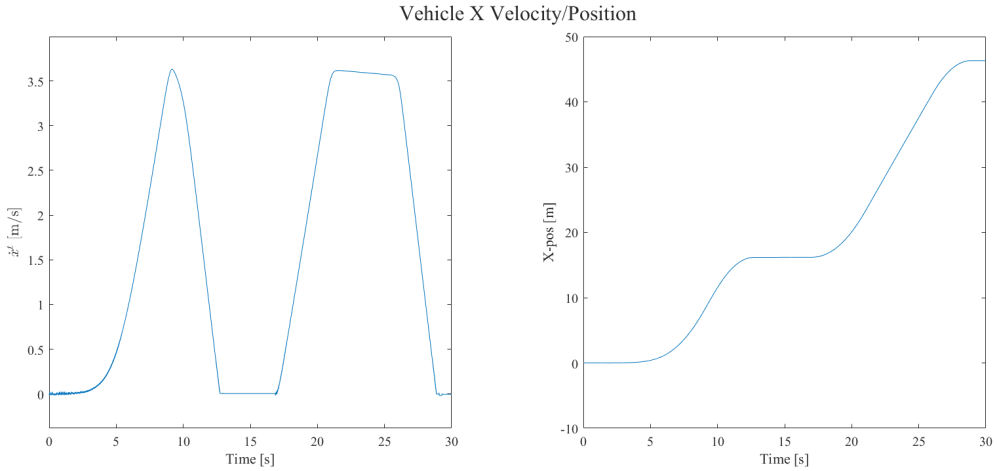

Figure 17: Bicycle Model Longitudinal Velocity and Position outputs

Note in the above figure how the aerodynamics drag causes the vehicle velocity to decrease when the engine set-point is released before the braking torque is applied again.

4.2.2 Step Steer Response

The following simulation displays the vehicle body's response to a step response steering input.

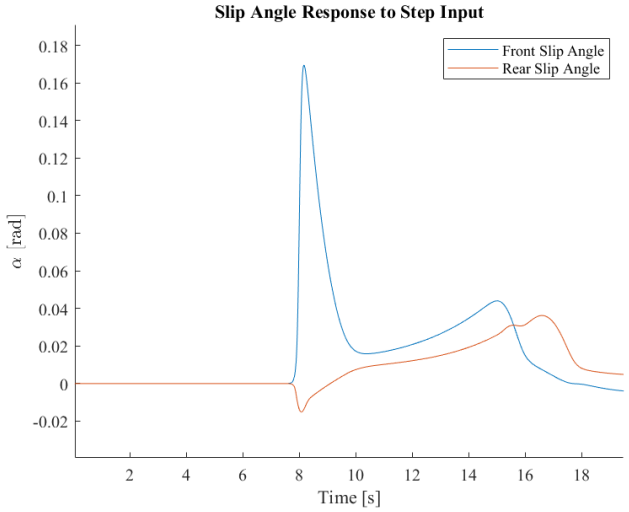

Figure 18: Slip angles response to step steering input with $\delta = 0.2$

We can also see the dynamic nature of the model by varying parameters such as the moment of inertia and observing the time response to the same steering input.

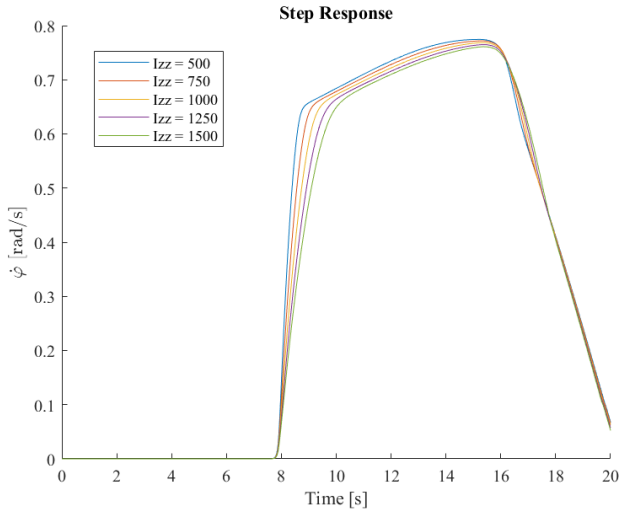

Figure 19: Yaw Rate response to step steer input with variable I_{zz}

Note that longitudinal velocity is not assumed constant in this simulation and is a product of throttle/braking set-points which are changing. As they are coupled, this results in a slightly different yaw rate output.

4.3 Multi-Axle Model

4.3.1 Combined Lateral/Longitudinal Inputs

The following simulation utilized a smoothed step function for the throttle and brake set-points in combination with a sin function with a frequency of $0.5 rad/s$ and an amplitude of $0.1 rad$ for the steering input δ_f.

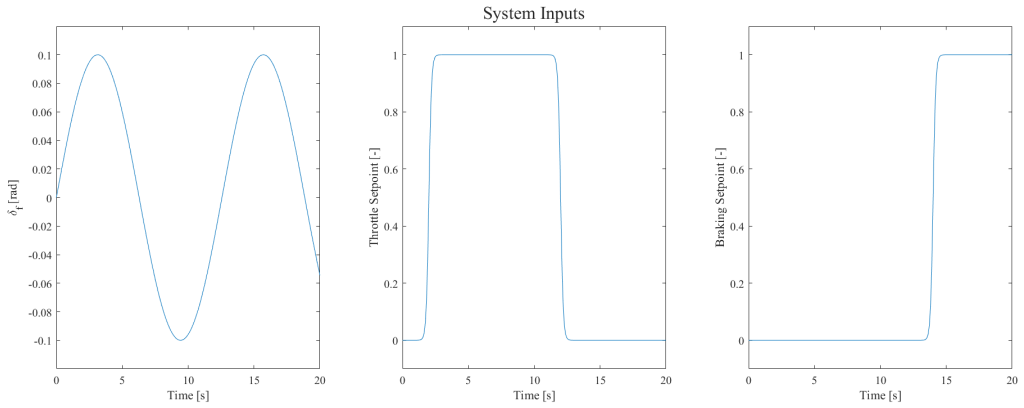

Figure 20: Coupled Model Simulation Inputs

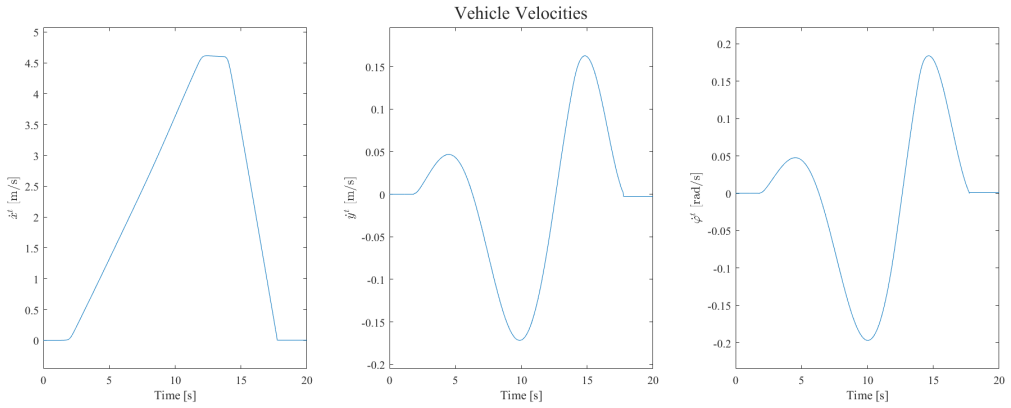

Figure 21: Vehicle Velocities output from coupled model

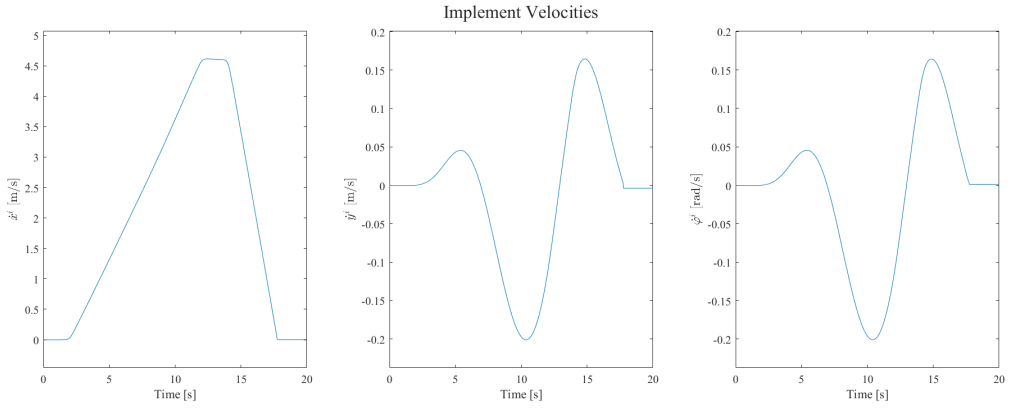

Figure 22: Implement velocities output from coupled model

4.3.2 Skidpad Maneuver

The following simulation was performed with identical throttle and braking set-points and a constant $\delta_f = 0.2$. Notice the intuitive behavior of the CG location of the implement relative to vehicle with the implement CG tracking inside of the radius of the vehicle.

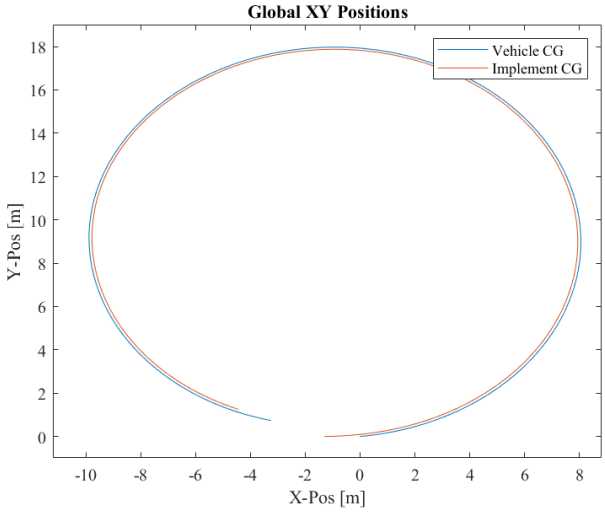

Figure 23: Vehicle and Implement CG Global CG Location

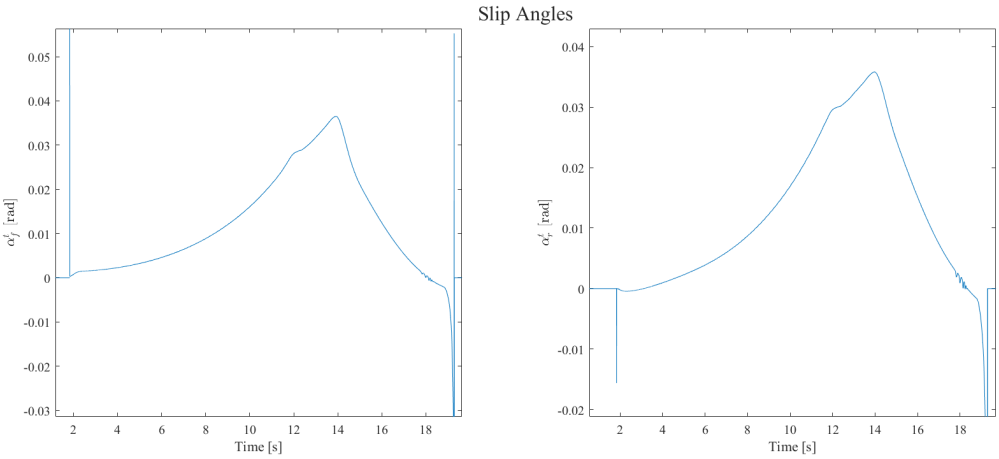

Figure 24: Vehicle slip angles during skid pad with variable longitudinal velocity.

Examining the slip angles allows us to see that the peak force generation exists at the point of highest longitudinal velocity. We can also see instances where the slip angles experience unexpected 'spikes' when the vehicles transitions to or from a zero velocity. More development will be needed to resolve this issue.